Time-resolved Dynamic Light Scattering as a Method to Monitor Compaction during Protein Folding

Klaus Gast*, Dietrich Zirwer, Gregor Damaschun

Max-Delbrück-Center for Molecular Medicine, Robert-Rössle-Str. 10,
D-13092 Berlin, Germany, PF 740238

Fax. +49 30 9406 2548, E-mail: gast@mdc-berlin.de

Summary: The mechanisms and the dynamics of protein folding are subject of a still increasing number of theoretical and experimental studies. While spectroscopic methods are already used for many years to measure the folding rates and to monitor the formation of secondary and tertiary structure, kinetic measurements of the compactness are only beginning to emerge. Time-resolved dynamic light scattering (DLS) is a useful tool to follow the compaction during protein folding by measuring the hydrodynamic Stokes radius R_S. Additionally, changes in the state of association can be detected by simultaneous measurements of the scattering intensity. The usefulness of different techniques for time-resolved DLS measurements and the general limits for kinetic DLS experiments are discussed first. Then we describe the adaptation of a stopped-flow system (SFM-3) to a DLS apparatus, the particular data acquisition schemes, and the experimentally attainable limits. The feasibility of stopped-flow DLS is demonstrated by the results of folding investigations with ribonuclease A, phosphoglycerate kinase, and bovine α-lactalbumin. Refolding was initiated by denaturant dilution jumps, which were repeated up to 100 times in order to obtain a reasonable signal-to-noise ratio. Kinetic DLS experiments can be performed fairly with a time resolution of one second. The time resolution of 100ms is probably the attainable limit. The capabilities of time-resolved DLS and time-resolved small-angle X-ray scattering are compared.

Introduction

Protein folding, the process by which a polypeptide chain folds into its functional three-dimensional structure, is one of the fundamental problems studied in structural biology [1, 2]. The structure of the folded protein, its stability, and how this structure is attained are encoded in the linear sequence of amino acids and depend on the specific environmental conditions [3].

 CCC 1022-1360/00/$ 17.50+.50/0

To find out general rules describing this process is the goal of researchers from different scientific fields. The starting point for protein folding experiments is an ensemble of unfolded conformations [4] obtained by subjecting the protein to extreme conditions such as high concentrations of denaturing agents, e.g., 6 M guanidinium chloride (GuHCl) or 8 M urea, extreme pH, high or low temperatures or high pressure. Folding is then initiated by a rapid jump to so-called native conditions and the structural changes are followed by different biophysical or biochemical techniques [2, 5]. Energetically and with respect to the observed folding rates, this process can be described in an elegant way by a folding funnel or an energy landscape [6, 7] showing the native state with the lowest free energy at the bottom of the funnel. The folding rate(s) and the complexity of folding routes depend on the ruggedness of the energy landscape. The hypothetical folding funnel does not reflect directly the changes on different structural levels occurring during folding. A variety of biophysical methods has to be used to describe the formation of the native structure [5]. Some aspects of structure formation, the methods used and typical attainable time-ranges are shown in Tab.1.

Tab. 1: Methods used to monitor structural changes during folding

Event	Methods	Time range
Formation of elements of regular secondary structure	Far-UV circular dichroism Fourier-Tr. IR spectroscopy	ms
Formation of persistent hydrogen-bonded secondary structure	Pulsed hydrogen-deuterium exchange combined with 2D NMR	ms
Formation of the hydrophobic core	Intrinsic and extrinsic fluorescence, UV absorption	ms (μs)
Side chain ordering and formation of native tertiary structure	Intrinsic fluorescence, near-UV circular dichroism real-time NMR	 ms s
Hydrophobic collapse and compaction of the polypeptide chain	Fluorescence quenching Small-angle X-ray scattering Dynamic light scattering	μs ms s

While optical spectroscopic methods have been used already many years for measuring the rates of folding and monitoring the formation of secondary and tertiary structure, only recently

methods measuring the size of the folding protein molecules directly have been emerged. This concerns small-angle X-ray scattering (SAXS) [8-10] and dynamic light scattering (DLS) [11-15]. Measuring the compactness of proteins during folding is important for several reasons, particularly in connection with the experimental verification of the predictions of different folding hypotheses and basic folding schemes [16-20]. There are two controversial views concerning basic folding events: the hierarchic or sequential folding scheme [16-18] and the hydrophobic collapse model [19, 20]. The latter model predicts a fast hydrophobic collapse as the initial step of folding, while within the sequential scheme chain collapse should occur concomitantly with the formation of secondary and tertiary structure. Time-resolved measurements of the molecular dimensions can thus help to answer the fundamental question, what folding scheme is preferred by a particular protein.

Initiation of folding reactions - useful techniques for time-resolved DLS

The potentials and problems of time-resolved DLS measurements will be discussed only in connection with protein folding, however, the general principles can be applied to any time-dependent process in solution, which can be studied preferentially by DLS.

Tab.2: Various techniques for initiating folding/unfolding reactions concerning attainable time ranges, required response of the detection method and applicability to DLS studies

Technique	Time range	Required response	Application notes for DLS
Manual mixing	> 10 s	medium, slow	useful only for $\Delta t > 1$min
Continuous-flow	> 10 µs	slow !	> 100ms*, used for $\Delta t > 1$s
Stopped-flow	> 3 ms	fast	> 100ms*, used for $\Delta t > 1$s
Quenched-flow	> 15 ms	slow	not suitable
Temperature jump	> 10ns/1µs/10s	very fast/fast	used for $\Delta t > 10$s
Pressure jump	> 50µs	fast	not tested

* estimated practical limit for DLS measurements

There are different ways, how a protein can be transferred from particular unfolding to folding conditions. This depends mostly on the protein under study, but on the chosen detection methods as well. Tab.2 shows some widely used techniques for the initiation of folding reactions. From these techniques, only the continuous-flow and stopped-flow methods will be

considered in more detail, although the use of fiber optics in DLS instrumentation [21] enables studies at sufficiently high pressure needed for pressure jump experiments. Temperature jumps were employed in our first kinetic DLS experiments [12], but this technique is restricted to special cases, for example, when cold-denaturation of proteins can be observed. In continuous-flow as well as in stopped-flow experiments refolding is initiated by diluting the denaturing agents with buffer.

Continuous-flow technique

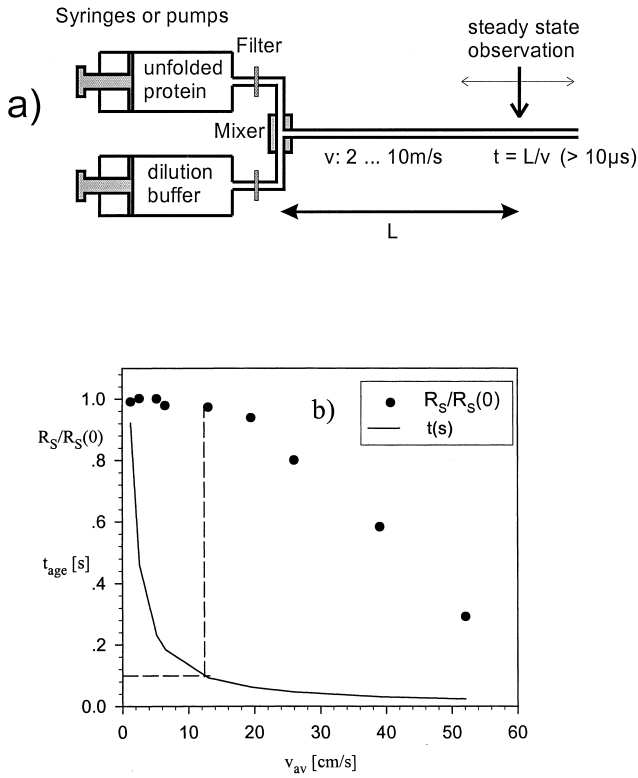

Fig.1: a) Continuous-flow apparatus, b) Influence of flow on the apparent Stokes radius

In a continuous-flow (CF) experiment (Fig.1a) the solution of unfolded protein and the buffer are contained in different mechanically or pneumatically driven syringes or medium pressure pumps. A special capillary mixer yielding fast mixing in a turbulent flow is used [10, 22-24]. The

"age" of the mixed solution is determined by the distance between the mixer and the position of observation and the velocity of the stream. CF has recently had a revival in protein folding because aging times as low as 10μs have been achieved. A further advantage is that even slow detection methods can be used provided there is enough material to maintain the stream for sufficiently long times. Membrane filters can be placed between the pumps and the mixer. But, the advantages of this technique mostly fade away in the case of DLS because the measurements have to be done in a flowing system. In flowing systems the measured intensity autocorrelation function is distorted by the uncorrelated replacement of scattering particles within the scattering volume. To check whether or not one can find a suitable compromise at appropriate flow velocities, we have performed measurements of the Stokes radius of bovine ribonuclease A (RNase A) under flow conditions using a small rectangular flow-through cell with 0.8mm optical pathlength. The results (Fig.1b) indicate that a noticeable decrease in the measured apparent Stokes radius is observed when the average velocity exceeds about 15cm/s. At this velocity and a typical distance of about 1cm between mixer and observation spot, aging times of the order of 0.1s could be achieved. This is hardly better than the expected time resolution of stopped-flow DLS measurements. Furthermore, it must be taken into consideration that CF measurements yield only one delay time in experiments with single detector arrangement. Enlarging the scattering volume would reduce the distortions due to flow but the signal-to-noise ratio too. However, this must be kept as high as possible in kinetic DLS experiments. A somewhat different CF scheme for delay times larger than 1s was used for kinetic DLS measurements by Feng et al. [11].

Stopped-flow technique

In a stopped-flow (SF) instrument (Fig.2), the experiment is started after stopping the mixing flow in an appropriate way. High quality of the stop is important for undistorted measurements. However, for SF measurements a fast detection and recording system is required. In general, the signal-to-noise ratio of a single record is too low for adequate data evaluation. In some cases, the measurement must be repeated up to several hundred times. The actual age of the mixed solution is the sum of the dead time caused by the flow time between mixer and observation spot and the aging time after the shot. SF systems are commercially available, and with modern devices the dead time can be reduced down to about 1ms. Nevertheless, for studies of the fastest processes of protein folding this time is even too

long. The temporal resolution after the dead time depends entirely on the particular method used. The attainable limits for DLS experiments are discussed in the following.

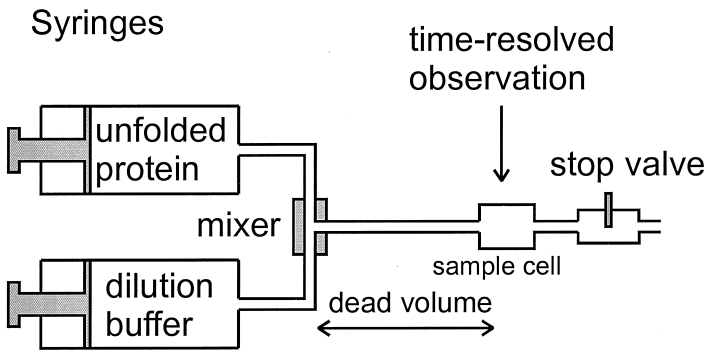

Fig.2: Stopped-flow apparatus

The speed-limit of time-resolved DLS experiments

Dynamic light scattering is not an intrinsically fast method. Here, we consider the special requirements for moderately fast measurements. It is important to perform simultaneous measurements of the time courses of the average scattered intensity I(t) and the Stokes radius $R_S(t)$ or the corresponding translational diffusion coefficient D(t), respectively. In this way, one can distinguish between true changes in the molecular size and those changes in R_S, which are influenced by association and dissociation of molecules. The experiments are performed at a fixed scattering angle of 90 deg.. Fortunately, proteins with $M_r < 200{,}000$ having Stokes radii < 10nm behave essentially like Rayleigh scatterers. For proteins, the correlation times τ_c of the first order correlation function $g^{(1)}(\tau)$ are within the range between 10 and 50 μs at temperatures near 20°C. It is evident that time-resolved measurements of the average intensity do not introduce any problems concerning the signal-to-noise ratio, even when the average is taken over time intervals as short as 1ms.

Several problems and limitations are connected with measurements of R_S. The shortest time interval T_A for obtaining an estimate of R_S in a single record is limited by the correlation time τ_c itself, and should be larger than about $1000 \cdot \tau_c$. This is the minimum time needed to obtain a reasonable time-averaged autocorrelation function. Accordingly, for proteins the shortest accessible time interval is only in the range between 10 and 50ms. This time is even longer for

larger particles. The temporal changes of R_S are recorded by calculating correlation functions during n_A equally spaced time intervals T_A after mixing. This yields a time resolution T_A and a total observation time $T_A \cdot n_A$. In order to achieve a sufficiently high signal-to-noise ratio (S/N), the measurement must be repeated n_S times, where n_S is the number of "shots" leading to a total data acquisition time $T_{A,tot} = T_A \cdot n_S$ and a total experiment time $T = T_A \cdot n_S \cdot n_A$. Only when the DLS experiment is performed well above the shot-noise limit, i.e. if the number of photon pulses per correlation time is >1, the attainable (S/N) is roughly proportional to $(T_{A,tot}/\tau_c)^{1/2}$. Otherwise the measurement time to obtain a good (S/N) is additionally prolonged. Therefore, high laser power and an efficient detection system are needed. However, a peculiarity of DLS becomes evident especially in kinetic experiments. For most of the other methods, the data acquisition time can be shortened by technical improvements. This is not further possible with DLS, if one has crossed the shot-noise limit. More detailed considerations concerning data acquisition times in kinetic DLS experiments based on calculations of Jakeman et al. [25] have been published in connection with our first kinetic DLS results [12]. In order to obtain sufficiently precise values of R_S, $T_{A,tot}$ should be $\geq$ 30s. It has to be shown, whether the estimated time resolution of the order of 50ms can be achieved experimentally with moderate effort.

Experimental set-up for stopped-flow DLS and data acquisition schemes

The basic components of our stopped-flow DLS apparatus are shown in Fig.3 and described in more detail elsewhere [13]. The mechanical basis is formed by a commercial stopped-flow system SFM-3 (Bio-Logic, France). This system is very flexible and is, therefore, suitable for an adaptation to a DLS spectrometer. The SFM-3 stopped-flow module contains 3 syringes and 2 mixers. The pistons of the syringes are driven independently by stepping motors allowing suitable mixing ratios over a wide range.

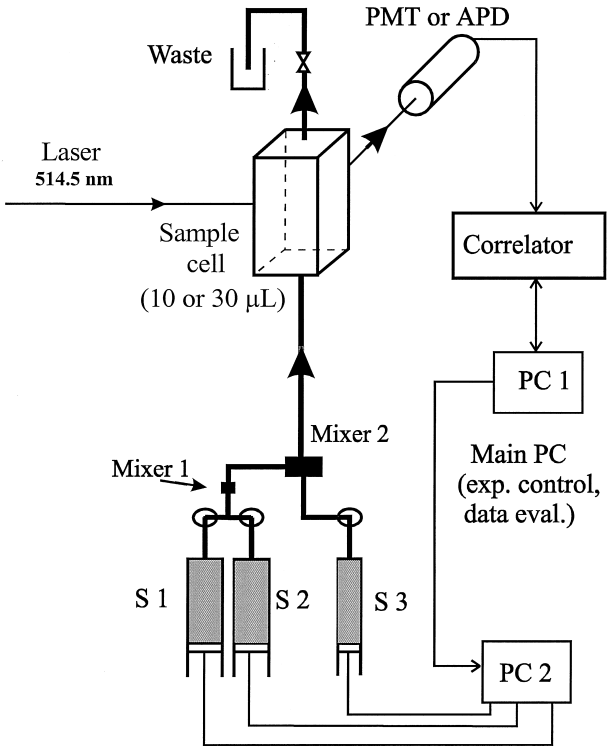

Fig.3: Stopped-flow DLS apparatus

The SFM-3 is controlled by a separate PC. Protein solution and buffer are mixed with mixer 2. We use rectangular cells with 0.8 and 1.5mm optical pathlength. The dead volume is 9µL or 31µL, respectively. We employ an argon laser Lexel 3500 (Lexel Laser, Inc., USA), mostly operating at 514.5nm and 0.5W output power. Until recently, the scattered light was detected by a photomultiplier tube PMT. With a new detection system based on an avalanche photodiode APD (ALV, Germany) the pulse-rate could be enhanced by a factor of 6 at constant laser power and amplitude of the normalized correlation function. By using the APD and 0.8mm sample cells, the amount of protein needed for kinetic experiments can be reduced considerably as compared to earlier experiments. A laboratory built multi-bit multiple-τ correlator is used. With this correlator, short acquisition times T_A of about 100ms can be obtained and an efficient kinetic DLS experiment can be programmed using the main PC1. PC1 sends trigger signals to PC2, which controls the mixing sequences of the SFM-3. The

most crucial point in stopped-flow DLS experiments is the avoidance of dust and gas bubbles. The entire stopped-flow apparatus must be purged with filtered water or buffer before use. To minimize the formation of bubbles, the system cannot be run at the highest possible mixing rate. Nevertheless, dead time of about 5ms can be reached.

Tab.3: Data acquisition scheme for a stopped-flow DLS experiment

scaling period	1. shot	1. acquis. T_A: file-01.001	2. acquis. T_A: file-01.002	. . .	n_A. acquis. T_A: file-01.n_A
	2. shot	1. acquis. T_A: file-02.001	2. acquis. T_A: file-02.002	. . .	n_A. acquis. T_A: file-02.n_A
		.	.		.
		.	.		.
	n_S. shot	1. acquis. T_A: file-n_S.001	2. acquis. T_A: file-n_S.002	. . .	n_A. acquis. T_A: file-n_S.n_A

Tab.3 shows the general data acquisition scheme. The actual experiment, after setting the data acquisition and averaging time T_A, the number of acquisitions after each shot n_A, the number of shots n_S, and performing a short scaling procedure, yields a relatively large array of $n_A \times n_S$ correlation functions, which are stored on the hard-disk. During the experiment, D(t) estimated by the cumulant method and I(t) are displayed after each shot as a graph on the monitor. Normally, a direct superposition of correlation functions belonging to the same time delay after a shot, i.e. all members of a column in Tab.3, is not possible because the data set contains distorted correlation functions. This results mostly from some unavoidable bubbles. A table of acceptable records is generated after the experiment allowing an appropriate data overlay and final data evaluation. If the solution indeed contained only protein monomers, a cumulant analysis is sufficient. In general, an inverse Laplace transformation using the program CONTIN [26, 27] must be performed to get $R_S(t)$.

Some applications of stopped-flow DLS to protein folding

The experimental time limit tested with RNase A

A dilution experiment with native buffer was used to check the reliable time range for stopped-flow DLS measurements of R_S of proteins. RNase A (M_r = 13,690) in 50mM sodium phosphate buffer, pH6, was eight-fold diluted to a final concentration of 0.9mg/mL. In this experiment, a constant Stokes radius and a constant scattering intensity should be observed after the dilution jump. The results are shown in Fig.4, which may also serve as an illustration of the experimental procedure.

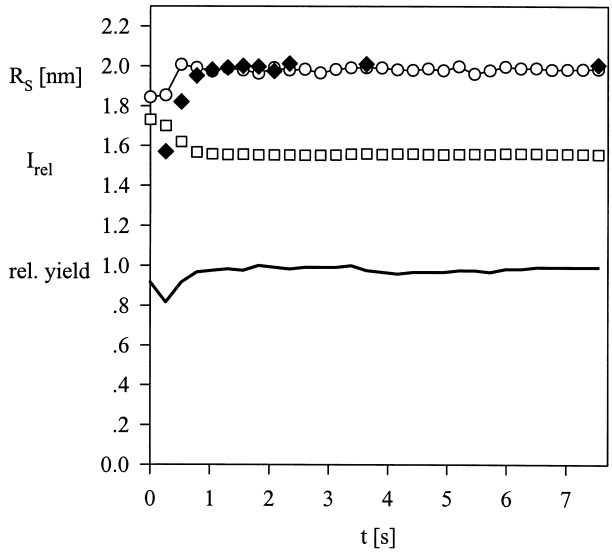

Fig.4: Stopped-flow dilution experiment with RNase A: 8-fold dilution with 50mM Na-cacodylate, pH6, T = 24°C, final protein concentration .91mg/mL, total number of "shots" = 120, Δt = 0.26s. —○— R_S(cumulant), ◆ R_S(CONTIN), □ I_{rel}, —— rel. yield

A total of 120 shots was performed. The lower trace in the figure indicates the relative yield. This is the proportion of undistorted measurements, which is normally about 0.8. In the present case, it is near to 1 and drops only slightly at times immediately after the shot. Correlation functions and average scattering intensities were obtained at 30 equally spaced delay times. The time increment $\Delta t = T_A$ was 0.26s. The coinciding Stokes radii, calculated by

either the cumulant method or inverse Laplace transformation, demonstrate that the system was monodisperse. Some distortions are observed for both the intensity and the Stokes radius at delay times $T_A \leq 0.5$s. This is probably due to an imperfect stop of the flow. The experiment demonstrates that measurements in the subsecond region are feasible, provided that the quality of the stop can be improved slightly, for example by installing a hard-stop valve behind the cuvette.

Refolding experiments with RNase A

On unfolding by 6M GuHCl, the Stokes radius of RNase A with the disulfide bonds intact increases from 1.95nm to 2.56nm. Refolding was initiated by a GuHCl concentration jump from 6M to 0.67M. It is known [28], that the majority of protein molecules folds slowly within the time range of seconds. The corresponding changes of the Stokes radius are shown in Fig.5.

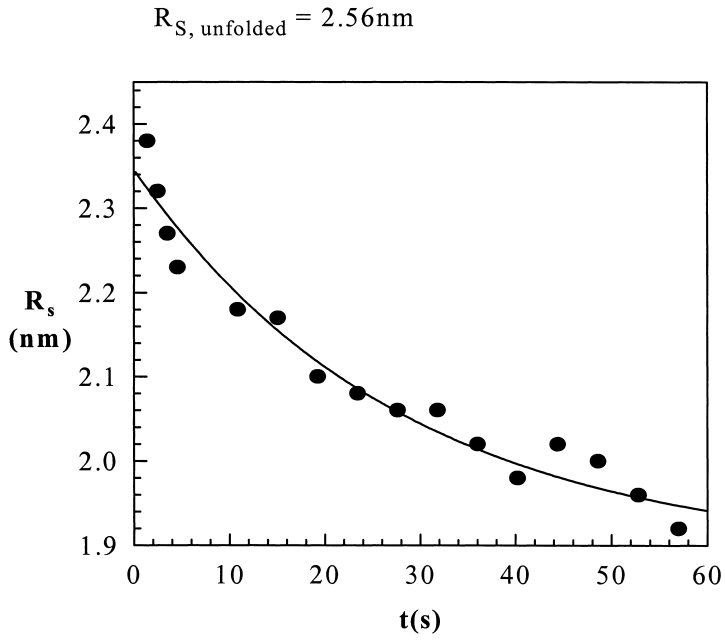

Fig.5: Refolding of RNase A measured by stopped-flow DLS

The special issue of the folding experiments with RNase A was a comparison of secondary structure formation measured by far-UV CD with the increase in compactness of the protein measured by DLS. From the results of both methods [14] the conclusion could be drawn that an initial hydrophobic collapse is not observed for RNase A. Secondary structure and compactness develop concomitantly during the late rate-limiting step of folding.

Refolding experiments with phosphoglycerate kinase

The refolding experiments with phosphoglycerate kinase (PGK) from yeast (M_r = 44,607) consider another important problem of protein folding, namely the relation between folding and association.

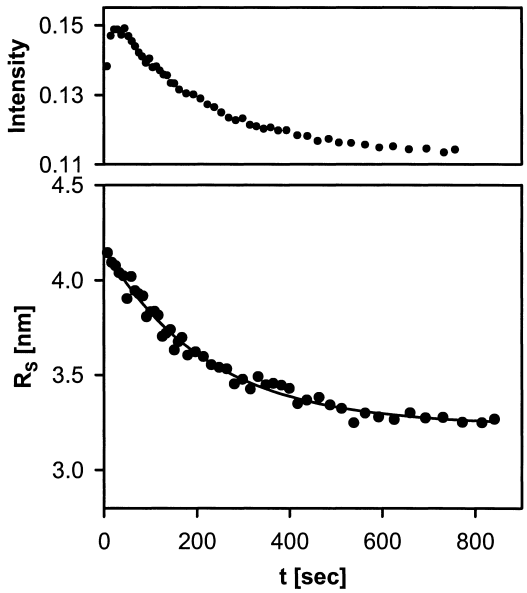

Fig. 6: Scattered intensity and R_S during refolding of PGK

Therefore, we have shown in Fig.6 the time courses of the scattered intensity and of the Stokes radius. The fast increase in the scattered intensity indicates that a folding intermediate is formed, which has the ability to associate. Interestingly, this ability is lost during further folding towards the native state. As a consequence, even the already existing aggregates

dissociate. In this experiment, the measured Stokes radius must be considered with special care because its changes result from both association/dissociation and conformational changes of the protein molecules.

Refolding experiments with bovine α-lactalbumin

α-lactalbumin (M_r = 14,186) is widely used as a model protein for folding studies. A particular folding intermediate, the so-called molten globule [29-31], has been detected in equilibrium folding/unfolding investigations. Much effort has been undertaken to demonstrate the close structural similarity between the intermediate state found in kinetic refolding experiments and the equilibrium molten globule state. Our stopped-flow DLS results confirm this hypothesis concerning the hydrodynamic dimensions [15]. Fig.7 shows that the relatively compact molten globule is formed within the dead time of the experiment and the compactness of the native state is reached within seconds.

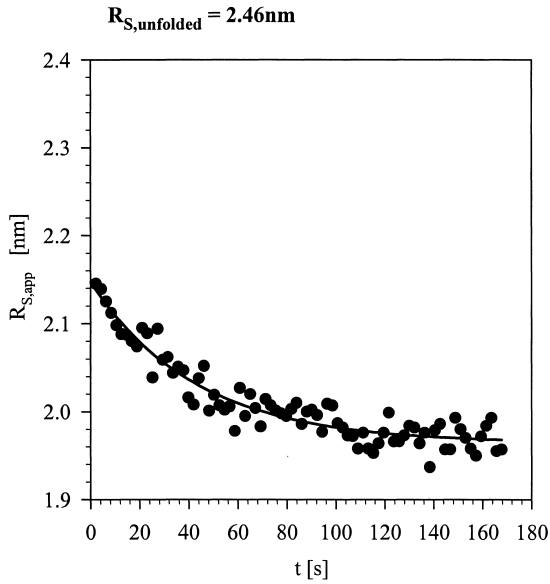

Fig.7: Stopped-flow kinetics of compaction of α-lactalbumin

The Stokes radius measured at finite protein concentration is only an apparent quantity. This is due to strong attractive intermolecular interactions of the kinetic molten globule reflected

by the strong concentration dependence of the diffusion coefficient. The concentration dependences for the kinetic molten globule, the native and the unfolded states are shown in Fig.8. Extrapolation to zero protein concentration yields a Stokes radius of the molten globule, which is only slightly larger than that of the native protein.

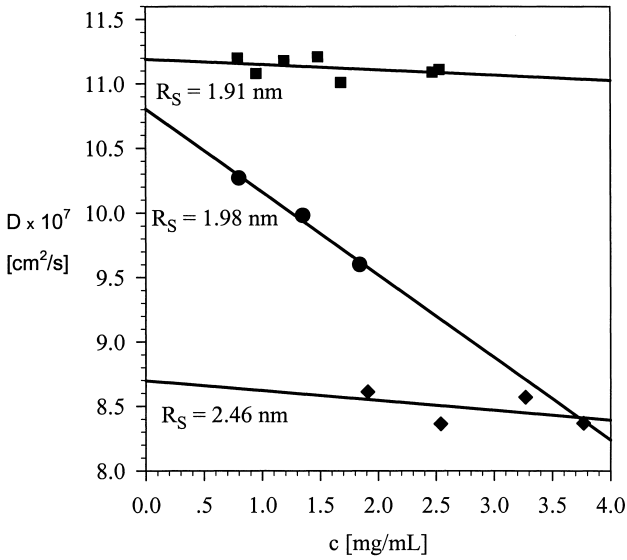

Fig. 8:
Concentration dependence of D in different states. The Stokes' radii were calculated from D extrapolated to c = 0.
■ native state ◆ unfolded state (5M GuHCl)
● kinetic molten globule

Conclusions

Our results demonstrate that kinetic DLS experiments yielding the Stokes radius and the molecular mass can be performed fairly with a time resolution of one second. Measurements below one second require special care and a resolution of 100ms is probably the attainable limit. The application of continuous-flow measurements, which has improved the time

resolution in connection with some other methods, is only of limited practical importance for DLS. Stopped-flow DLS requires high quality of the mixing and stopping procedures, laborious purging of the entire stopped-flow system and a careful preparation of the solvents. It is worth and important to compare the capabilities of time-resolved DLS experiments with those of time-resolved SAXS. Basically, the latter experiments are much more difficult to perform because a high X-ray photon flux is needed, which is only available at synchrotron stations. However, the information content of time-resolved X-ray data is higher since geometric quantities, the radius of gyration R_G and the distance distribution function P(R), can be obtained directly [9]. Furthermore, these measurements can be performed with high velocity flows, and filtration of the sample is not essential. On the other hand, lower concentrations, for example final concentrations of about 1mg/mL in the case of proteins, can be used in time-resolved DLS experiments. This is very important for the proper correction of virial influences (see Fig. 8).

Acknowledgements

This work was supported by grants from the Deutsche Forschungsgemeinschaft (Da292/6-2, He1318/18-2) and by a grant from the Fonds der Chemischen Industrie to G. D..

References

1. C. M. Dobson, M. Karplus, Curr. Opinion Struct. Biol. **9**, 92 (1999)
2. O. Bieri, T. Kiefhaber, Biol. Chem. **380**, 923 (1999)
3. C. B. Anfinsen, Science **181**, 223 (1973)
4. G. Damaschun, H. Damaschun, K. Gast, D. Zirwer Biochemistry (Moscow) **63**, 259 (1999)
5. K. W. Plaxco, C. M. Dobson, Curr. Opinion Struct. Biol. **6**, 630 (1996)
6. J. D. Bryngelson, J. N. Onuchic, N. D. Socci, P. G. Wolynes, Proteins: Struct. Funct. Genet. **21**, 167 (1995)
7. K. A. Dill, Protein Sci. **8**, 1166 (1999)
8. L. Chen, G. Wildegger, T. Kiefhaber, K. O. Hodgson, S. Doniach, J. Mol. Biol. **276**, 225 (1998)
9. D. J. Segel, A. Bachmann, J. Hofrichter, K. O. Hodgson, S. Doniach, T. Kiefhaber, J. Mol. Biol.. **288**, 489 (1999)
10. L. Pollack, M. W. Tate, N. C. Darnton, J. B. Knight, S. M. Gruner, W. A. Eaton, R. H. Austin, Proc. Natl. Acad. Sci. USA **96**, 10115 (1999)
11. H.-P. Feng, D. S. Scherl, J. Widom, Biochemistry **32**, 7824 (1993)
12. K. Gast, G. Damaschun, R. Misselwitz, D. Zirwer, Eur. Biophys. J. **21**, 357 (1992)
13. K. Gast, A. Nöppert, M. Müller-Frohne, D. Zirwer, G. Damaschun, Eur. Biophys. J. **25**, 211 (1997)

14. A. Nöppert, K. Gast, D. Zirwer, G. Damaschun, Fold. Des. **3**, 213 (1998)
15. K. Gast, D. Zirwer, M. Müller-Frohne, G. Damaschun, Protein Sci. **7**, 2004 (1998)
16. P. S. Kim, R. L. Baldwin, Annu. Rev. Biochem. **51**, 459 (1982)
17. R. L. Baldwin, G. Rose, Trends Biochem. Sci. **24**, 26 (1999)
18. R. L. Baldwin, G. Rose, Trends Biochem. Sci. **24**, 77 (1999)
19. K. A. Dill, Biochemistry **24**, 1501 (1985)
20. K. A. Dill, S. Bromberg, k. Yue, K. M. Fiebig, D. P. Yee, P. D. Thomas, H. S. Chan, Protein Sci. **4**, 561 (1995)
21. S. Zhou, B. Chu, H. S. Dhadwal, Rev. Sci. Instrum. **69**, 1955 (1999)
22. J. B. Knight, A. Vishwanath, J. P. Brody, R. H. Austin, Phys. Rev. Lett. **80**, 3863 (1998)
23. P. Regenfuss, R. M. Clegg, M. J. Fulwyler, F. J. Barrantes, T. M. Jovin, Rev. Sci. Instrum. **56**, 283 (1985)
24. M. C. R. Shastry, S. D. Luck, H. Roder, Biophys. J. **74**, 2714 (1998)
25. E. Jakeman, E. R. Pike, S. Swain, J. Phys. A **4**, 517 (1971)
26. S. W. Provencher, Comp. Phys. Commun. **27**, 213 (1982)
27. S. W. Provencher, Comp. Phys. Commun. **27**, 229 (1982)
28. F. X. Schmid, Biochemistry **22**, 4690 (1983)
29. K. Kuwajima, Proteins: Struct. Funct. Genet. **6**, 87 (1989)
30. O. B. Ptitsyn, in: *Protein Folding,* T. E. Creighton (Ed.), Freeman and Company, New York 1992, p.243ff
31. K. Kuwajima, FASEB J. **10**, 102 (1996)